Optical properties of dissolved organic matter connnect to different depth-related patterns of archaeal and bacterial community structure in the north Atlantic ocean”

Elisa Guerrero-Feijóo[1*], Mar Nieto-Cid[2], Vladimir Dobal-Amador[3], Víctor Hernando-Morales[4], Eva Sintes[5], Marta Álvarez[1], Vanessa Balagué[6] and Marta M. Varela[1].

[1]IEO, Instituto Español de Oceanografía, 15001, A Coruña, España.
[2]IIM-CSIC, Instituto de Investigacións Mariñas, 36208 Vigo, Spain.
[3]Departamento de Bioquímica, Xenética e Inmunoloxía, Universidade de Vigo, 36200 Vigo, Spain.
[4]Departamento de Ecoloxía e Bioloxía Animal, Universidade de Vigo, 36200 Vigo, Spain.
[5]Department of Limnology and Bio-Oceanography, University of Vienna, A-1090, Vienna, Austria.
[6]ICM-CSIC, Institut de Ciències del Mar, 08003, Barcelona, Spain.

Corresponding author:
Elisa Guerrero-Feijoo, Instituto Español de Oceanografia (IEO), Paseo Alcalde Fco. Vázquez 10, 15001, A Coruña, Spain. E-mail: elisa.guerrero.feijoo@gmail.com

ABSTRACT

Abundance, activity and prokaryotic community composition were studied in the euphotic, intermediate and deep waters off the Galician coast (NW Iberian margin) in relation to the optical characterization of dissolved organic matter (DOM). Microbial (Archaea and Bacteria) community structure was vertically stratified. Among the Archaea, Euryarchaeota, especially Thermoplasmata, was dominant in the intermediate waters and decreased with depth, whereas marine Thaumarchaeota, especially Marine Group I, was the most abundant archaeal phyla in the deeper layers. The bacterial community was dominated by Proteobacteria through the whole water column. However, Cyanobacteria and Bacteroidetes occurrence was considerable in the upper layer and SAR202 was dominant in deep waters. Microbial composition and abundance were not shaped by the quantity of dissolved organic carbon, but instead they revealed a strong connection with the DOM quality. Archaeal communities were mainly related to the fluorescence of DOM (which indicates respiration of labile DOM and generation of refractory sub-products), while bacterial communities were mainly linked to the aromaticity/age of the DOM produced along the water column. Taken together, our results indicate that the microbial community composition is associated to the DOM composition of the water masses, suggesting that distinct microbial taxa have the potential to use and/or produce specific DOM compounds.

INTRODUCTION

Marine microbes are major components of plankton and play a significant role in the oceanic biogeochemical cycles. Prokaryotic abundance and activity decrease with depth by one and two orders of magnitude, respectively (Arístegui et al. 2009; Furhman et al. 2015). Such pattern is determined by the vertical variability of the physical and chemical features of the pelagic environment, which also contribute to the vertical stratification of the microbial community composition (DeLong et al. 2006; Martín-Cuadrado et al. 2007; Agogué et al. 2011).

Sequencing (Sanger and 454 pyrosequencing) of rRNA gene is a valuable tool to characterize the microbial community structure in the water column (Giovannoni et al. 1996; DeLong et al. 2006; Yokokawa et al. 2010; Agogué et al. 2011; Lekunberri et al. 2013). Based on these techniques, several recent investigations have shown a vertical stratification of the microbial populations in the deep waters of the Atlantic Ocean (Agogué et al. 2011; Lekunberri et al. 2013; Ferrera et al. 2015, Frank et al. 2016) and Pacific Ocean (Schmidt et al. 1991; DeLong et al. 2006). In addition, variations of Archaea and Bacteria relative abundances among different water masses have also been well established by Catalyzed Reporter Deposition Fluorescence In Situ Hybridization (CARD-FISH) enumeration of specific phylogenetic groups. CARD-FISH studies revealed increasing relative abundance of archaeal cells with depth while Bacteria shows the opposite pattern (Karner et al. 2001; Teira et al. 2006; Varela et al. 2008a, 2008b; Dobal-Amador et al. 2016). Similarly, the distribution of specific groups of Bacteria varies considerably with depth (Varela et al. 2008b; Lekunberri et al. 2013, Doval-Amador et al. 2016). However, variation of the microbial community's composition with depth is not only attributable to the most abundant taxa, but also to the less abundant phylotypes. Recent results from next generation sequencing of the 16S rRNA gene indicate the existence of microbial phylotypes specific to the deep water masses of the Atlantic Ocean (Agogué et al. 2011; Ferrera et al. 2015).

Temperature, hydrostatic pressure and salinity correlate with the variation in abundance, activity and diversity of the microbial communities (Sjöstedt et al. 2014; Fuhrman et al. 2015, Doval-Amador et al. 2016). The amount and quality of organic matter in marine ecosystems is also recognized as a major factor that affects the metabolism, distribution and dynamics of prokaryotic communities (Cottrell and Kirchman, 2000; Kirchman et al. 2004; Dobal-Amador et al. 2016). However, our knowledge on the sources of DOM in the intermediate and deep waters and the link between the composition and diversity of DOM and microbial communities, particularly Archaea, in the dark ocean is still limited.

The Galician coast (NW Spain) is a dynamic area characterized by seasonal upwelling pulses, which support the exportation offshore and sinking of organic matter. Hence, this ecosystem represents an ideal study area to investigate how the composition and diversity of DOM might shape the microbial communities. Results from a previous exploratory study in the same area indicated that the bacterial community structure assessed by ARISA fingerprinting was related not only with physicochemical parameters but also by DOM quality (Dobal-Amador et al. 2016). The aim of the present study was to extend these previous results and investigate the role of DOM quality and quantity in shaping the archaeal community structure as compared to Bacteria, by using T-RFLP/ARISA fingerprinting and sequencing of the bacterial and archaeal 16S rRNA gene, along a longitudinal section off the eastern north Atlantic. We hypothesized that vertical variation in the different indices of the DOM results in different depth-related patterns in archaeal community structure as compared to Bacteria. We used the distance-based multivariate analysis for a linear model (DISTLM) and redundancy analysis (RDA) to identify the best set of optical properties of organic matter explaining the variations in the Archaea community structure and composition as compared to Bacteria in the euphotic, intermediate and bathypelagic waters of the eastern north Atlantic.

MATERIAL AND METHODS

Sampling

Sampling was conducted during the cruises BIO-PROF-1 (August 11th – 28th, 2011) and BIO-PROF-2 (September 11th – 20th, 2012), on board R/V Cornide de Saavedra from 43ºN, 9ºW to 43ºN, 14ºW off Cape Finisterre (NW Spain) (Fig. 1). Samples were collected with Niskin bottles mounted on a CTD (conductivity-temperature-depth) rosette sampler from different depths based on their temperature and salinity: euphotic zone (EZ, 3 samples, 5, 50 and 100 m depth); Eastern North Atlantic Central Water (ENACW, 2 samples, 250-300 and 500-900 m depth), the layer of the oxygen minimum zone (OMZ, ≈900m); Mediterranean Water (MW, 1 sample, 1000 m depth); Labrador Sea Water (LSW, 1 sample, 1800 m depth); Eastern North Atlantic Deep Water (ENADW, 1 sample, 2750 m depth) and Lower Deep Water (LDW, 1 sample, >4000 m depth). A total of 43 stations were sampled (22 and 21 stations for BIO-PROF-1 and BIO-PROF-2, respectively) to perform the physical and chemical analysis (Fig. 1). Seawater from six stations (5, 8, 11, 16, 108, 111, Fig. 1) were collected for dissolved organic matter measurements, and four stations (11, 16, 108 and 111, Fig. 1) were additionally sampled for microbial analysis, including abundance, activity, structure and composition of the prokaryotic communities in both cruises.

Chemical analysis

Samples for the analysis of dissolved oxygen measurements were collected in pyrex “iodine titration” flasks with flared necks and ground glass stoppers, with a nominal volume of about 115 mL. Following Langdon (2010), the samples were measured by the winkler potentiometric method. Nutrient salts (nitrate, nitrite, phosphate and silicate) were collected in rinsed polyethylene bottles and frozen at -20 ºC until further analysis by standard colorimetric methods on a segmented flow analyser Bran-Luebbe analyser following the procedures of Hansen and Koroleff (1999).

All DOM samples above 200 m were filtered under positive pressure using an acid-clean all-glass system and combusted (450 ºC, 4 h) GFF filters. Water samples for the analysis of dissolved organic carbon (DOC) were collected in combusted (450 ºC, 12h) glass ampoules, and acidified with H_3PO_4 to pH <2. The ampoules were heat-sealed and DOC was determined with a Shimadzu TOC-CSV analyser by high temperature Pt-catalytic oxidation (Alvarez-Salgado and Miller, 1998). DOM fluorescence intensity was measured on board within 2-3 hours at two pair of fixed excitation/emission wavelengths: 320 nm/410 nm (FDOM-M), characteristic of marine “refractory” humic-like substances; and 280 nm/350 nm (FDOM-T), characteristic of “labile” protein-like materials, using a Perkin Elmer LS55 following Nieto-Cid et al. (2006). Samples were calibrated against quinine sulphate and results are given in quinine sulphate units (QSU). UV-visible absorption spectra of the chromophoric DOM were acquired on a Beckman Coulter DU800 spectrophotometer equipped with 10cm quartz cuvettes also in a time frame of 2-3 hours after collection. Spectral scans were recorded from 250 to 700 nm, using the sample average absorbance between 600 and 700 nm to correct for offsets (Green & Blough, 1994). Absorption coefficients were calculated following Green & Blough (1994) at several wavelengths along the spectra aCDOM254 (absorption coefficient at 254 nm), aCDOM340 (absorption coefficient at 340 nm), and aCDOM365 (absorption coefficient at 365 nm). Differences between these indices lay on the nature of the colored DOM, as the intensification of the conjugation/aromaticity increases with the absorption wavelength (Stedmon & Nelson, 2015). Thus, absorption coefficients at wavelength larger than 300 nm would only gather information of complex/aromatic molecules and would not be related to relatively simple compounds. In addition, the shape of the absorption spectra was explored by means of the spectral slopes between 275 and 295 nm (sCDOM275-295), calculated from the linear regression of log-transformed absorption spectra, and providing information on shifts in molecular weight and DOM aromaticity (Helms et al, 2008). In general terms, absorption coefficients are considered "quantitative" variables, as they are a proxy of the concentration of colored DOM, while the slope of the spectra is assessed as a "qualitative" variable, indicating changes in colored DOM composition (Stedmon and Nelson, 2015).

Prokaryotic abundance

Following Gasol et al. (1999) samples for prokaryotic abundance (PA) were determined by flow cytometry. A volume of 1.8 mL per water sample was preserved with 1% paraformaldehyde (final concentration), shock-frozen in liquid N_2 for 10 min and stored at -80 ºC. Samples were thawed to room temperature and stained with Syto13 (Life Technologies) in the dark for 10 min. Subsequently, 1 µm fluorescent latex beads (approximately $1x10^5$ mL^{-1}) (Molecular Probes, Invitrogen, Carlsbad, CA) were added to all the samples as internal standard. The prokaryotes were counted using a FACSCalibur flow cytometer (Becton Dickinson, Franklin Lakes, NJ) according to their signature in right angle light scatter and green fluorescence.

Leucine incorporation rates

Leucine incorporation (Leu incorp.) rates from the microbial communities from the euphotic and upper intermediate waters (up to 500m) were measured by adding 5 nmol L^{-1} [^{3}H]-leucine (final concentration, specific activity 160 Ci mmol L^{-1}, GE Healthcare, Amersham, Bucks, UK) to triplicate 1.2 mL samples. Duplicate TCA (trichloroacetic acid)-killed blanks (5% final concentration) were treated in the same way as the samples (Simon and Azam, 1989). Samples and blanks were incubated in the dark and in situ temperature in temperature-controlled chambers for 2–6 h, depending on the expected activity. Incubations were terminated by adding TCA (5% final concentration) to the samples. Bacterial proteins were precipitated by two successive centrifugation steps (12000 rpm, 10 min), including a washing step with 1 mL of 5% TCA following Kirchman (1985) with slight modifications (Smith and Azam, 1992).

Leu incorp. from the lower intermediate and deep waters (below 1000m) was determined by adding 5 nmol L^{-1}[^{3}H]-leucine (final concentration, specific activity 160 Ci mmol L^{-1}, GE Healthcare, Amersham, Bucks, UK) to duplicate 40 mL samples and duplicate formaldehyde-killed blanks (2% final concentration) (Simon and Azam, 1989). The incubation of samples and blanks was carried out in the dark and in situ temperature for 10 - 24 h, depending on the expected activity. The incubations were finished by adding formaldehyde (2% final concentration) to the samples. Samples and blanks were filtered onto 0.2 µm polycarbonate filters (25 mm filter diameter, Millipore). Afterwards, the filters were rinsed with 10 mL 5% ice-cold TCA and air-dried before liquid scintillation cocktail was added to the vials. After 18 h, the radioactivity was quantified in a scintillation counter (LBK Wallac). The disintegrations per minute (DPMs) of the blanks were subtracted from the mean DPMs of the respective samples and the resulting DPMs converted into leucine incorporation rates. The cell-specific activity was estimated dividing Leu incorp by PA.

DNA extraction of the prokaryotic community

A volume of 10 - 15 L of water was filtered through sterile Sterivex 0.22 µm pore size filters (Millipore, USA). 1.8 mL of lysis buffer (40 mM EDTA, 50 mMTris-HCl, 0.75 M sucrose) was added to the filter cartridge and stored at -80 ºC. DNA extraction was performed by enzymatic lysis of the cells with lysozyme and proteinase K, followed by phenol-chloroform extraction. DNA was precipitated by the addition of isopropanol. The pellet was washed with 70% ethanol and resuspended in sterile TE buffer. DNA samples were quantified and quality checked (according to the A260/A280 ratio) using a Nanodrop spectrophotometer (Thermo Scientific, USA).

T-RFLP and ARISA fingerprinting of archaeal and bacterial communities

Two different fingerprinting techniques, T-RFLP and ARISA, were performed to study archaeal and bacterial community structure, respectively. Both techniques can be used to quickly profile the structure of microbial communities. The ITS region used for ARISA is more variable than the 16S rRNA used for T-RFLP. Slightly higher total numbers of bacterial OTUs have been obtained with ARISA as compared to T-RFLP (Yokokawa et al., 2010). Thus, ARISA has been suggested to be more effective than T-RFLP on the 16S rRNA for estimating diversity of prokaryotic assemblages (García-Martínez et al. 1999) However, several Archaea harbours very short or even lack intergenic transcribed spacer (Moreira et al., 2004, Leuko et al., 2006). Taking these previous findings into account, we used ARISA fingerprinting to assess the bacterial community structure and T-RFLP was performed to assess the archaeal community structure.

T-RFLP fingerprinting was carried out on a standard amount of DNA (2 µL) from each sample by using the primer set 27F-FAM (FAM-6'-AGA GTT TGA TCC TGG CTC AG-3') and 958R-VIC (VIC-5'-YCC GGC GTT GAM TCC ATT T-3'; DeLong, 1992). PCR conditions and chemicals were applied as described by Moeseneder et al. (2001). PCR product was purified and subsequently digested at 37 ºC overnight with the tetrameric restriction enzyme (HhaI). The restriction enzyme was heat inactivated and the digested DNA was precipitated. Fluorescently labelled fragments were separated and detected in an ABI Prism 310 capillary sequencer (Applied Biosystems). The internal size standard used were LIZ 1200 (20-1200 pb, Applied Biosystems). The output from the ABI Genescan software was analysed with the FINGERPRINTING II software (BIO-RAD) to determine the peak height.

Automated rRNA intergenic spacer analysis (ARISA)-PCR was conducted on a standard amount of DNA (2 µl) from each sample. Bacterial ARISA was performed using ITSF, 5´-GTC

GTA ACA AGG TAGGCC GTA-3´, and ITSReub, 5´-GCC AAG GCA TCC ACC 3´, primer set (Thermo Scientific) as previously described (Cardinale et al. 2004). ARISA fingerprinting conditions have been previously reported (Dobal-Amador et al. 2016). ARISA fragments were separated using the ABI Prism 3730XL (Applied Biosystems) genetic analyzer applying the internal standard LIZ 1200 (20 – 1200 pb, Applied Biosystems). Obtained peaks with height value <20 fluorescence units were removed from the output peak matrix before statistical analyses. Each ARISA peak was defined as a different operational taxonomic unit (OTU).

Pyrosequencing of the archaeal and bacterial 16S rRNA gene

Pyrosequencing was performed for Archaea and Bacteria only at station 111 during the BIO-PROF 2 cruise. We analysed 7 samples, representative of the different water masses in this region. A subsample of the DNA extracted was used for pyrosequencing at the Research and Testing Laboratoy (Lubbock, TX, USA: http://medicalbiofilm.org) using 454 GL FLX technology. The Bacteria specific primers 28F (5'GAGTTTGATCNTGGCTCAG) and 519R (5'GTNTTACNGCGGCKGCTG) were used to generate amplicons from V1 to V3 regions of the bacterial 16S rRNA gene (~500 bp). Archaeal specific primers 341F (5'-GYGCASCAGKCGMGAAW-3') and 958R (5'-GGACTACVSGGGTATCTAAT-3') were used to amplify the region spanning the V3 to V5 regions (~600 bp). Subsequent analyses were performed using Quantitative Insights Into Microbial Ecology (QIIME) pipeline (http://qiime.org) (Caporaso et al. 2010).

A quality check was performed to minimize low quality pyrotags, eliminating sequences with 50bp sliding window Phred average below 25, ambiguous bases and sequences with length <100-125 bp after trimming. The remaining sequences were run into Denoiser to detect the pyrosequencing errors (Reeder and Knight, 2010). The curated sequences were grouped into operational taxonomic units (OTUs) with a 97% similarity threshold. A representative sequence from each phylotype was chosen by selecting the most abundant sequence in each cluster. MOTHUR was used to remove chimeras by ChimeraSlayer (Schloss 2009; Haas et al. 2011) based on the alignment file SILVA 108 (http://www.arb-silva.de). Blast Classifier (Wang et al. 2007) implemented in QIIME determined the identity of 16S rRNA phylotypes. OTUs assigned to chloroplast or mitochondria were removed from our analysis. In addition, the rarefraction curves were plotted to verify that the sequences obtained in each sample showed a tendency of plateauing for the most samples of Archaea (Fig. S1a) and Bacteria (Fig. S1b). Pyrotag sequences have been deposited in the National Center for Biotechnology Information (NCBI) Sequence Read Archive (SRA) under PRJNA317990 and PRJNA318014 bioproject numbers.

One OTU table was built for Archaea and another one for Bacteria. Both tables were subsampled to ensure an equal number of sequences per sample (1436 and 3511sequences for Archaea and Bacteria, respectively).

CARD-FISH and FISH

CARD-FISH was used to quantify the abundance of the major of prokaryotic groups at four stations (11, 16, 108 and 111) following the method described by Pernthaler et al. (2002). Immediately after collecting the samples from the Niskin bottles, 20–80 mL of seawater were preserved with paraformaldehyde (2% final concentration) and stored at 4 °C in the dark. About 12–18 h later, the samples were filtered onto 0.2 µm polycarbonate filters (Millipore GTTP, 25-mm filter diameter) supported by nitrocellulose filters (Millipore, HAWP, 0.45 µm), washed twice with 10 mL Milli-Q water, dried and stored in a microfuge vial at -20 °C until furtheranalysis. Filters were cut in sections and hybridized with horseradish peroxidase (HRP)-labelled oligonucleotide probes (Table S1), followed by tyramide-Alexa488 signal amplification. Cells were counter-stained with a DAPI-mix [5.5 parts of Citifluor (Citifluor), 1 part of Vectashield (Vector Laboratories) and 0.5 parts of phosphate-buffered saline (PBS) with DAPI (final concentration 2 μgmL^{-1})]. Quantification of DAPI-stained cells and cells stained with the specific probes was carried out under a Nikon Eclipse 80i epifluorescence microscope equipped with Hg lamp and appropriate filter sets for DAPI, Cy3 and Alexa448. A minimum of 500 DAPI-stained cells was counted per sample.

Statistical Analysis

All t-test analysis was performed using Sigmaplot 8.0. Hierarchical cluster analysis (CLUSTER) was carried out to explore similarities between samples, based on Bray-Curtis similarity matrix obtained by T-RFLP and ARISA fingerprintigs of archaeal and bacterial communities. Significant differences in microbial community composition between samples were investigated by permutational analysis of variance with PRIMER software (Primer-E v. 6; Anderson et al. 2001). The differences in alpha diversity among water masses (by using the 454 pyrosequencing data) were tested statically using ANOSIM analysis of the PRIMER software.
A distance-based linear model (DistLM) analysis was used to study the relationship between the resemblance matrix of microbial community structure and DOM-related variables. Previously, all variables were tested for co-linearity (Spearman correlation matrix) and those with determination coefficients (R^2) higher than 0.95 were eliminated. The contribution of each variable was assessed, firstly using “marginal test” to assess the statistical significance and percentage contribution of each variables taken separately. Secondly, a “sequential test” was employed to evaluate the cumulative effect of each variable once the previous variable(s) had

been accounted for. All variables were introduced in the model with the "step wise" selection procedure of the DistLM model, using the "Akaike" information criterion (AIC). Such procedure allows us to find the best combination of variables that explain the variability from the microbial resemblance matrix. All statistical tests were performed with PRIMER6 & PERMANOVA+ (Anderson et al. 2008). In addition, a redundancy analysis (RDA) was performed to examine the associations among DOM-variables and specific microbial groups obtained using 454-pyrosequencing with XLSTAT software.

RESULTS

Environmental parameters

The main water masses along a section off the Galician coast (Fig. 1) were identified according to their temperature and salinity signals (Prieto et al. 2013). The physical and chemical characteristics of these water masses are summarized in Table 1. No significant differences were detected for the physico-chemical variables among the two cruises (t-test, $p>0.5$, $n=555$ for temperature, salinity and oxygen; t-test, $p>0.5$, $n=371$ for nitrate, silicate and phosphate). The Lower Deep Water (LDW) was found below 4000 m depth. LDW is characterized by low temperature (2.5 ºC; Table 1), low salinity (34.4; Table 1), high dissolved oxygen (250 µmol kg^{-1}; Fig. S2a, S2b), nitrate (20 µmol kg^{-1}; Fig. S2c, S2d), phosphate (1.5 µmol kg^{-1}; Fig. S2e, S2f) and silicate concentration (32.8 – 44.94 µmol kg^{-1}; Fig. S2g, S2h). The Eastern North Atlantic Deep Water (ENADW) was identifiable by slightly higher temperature (2.5 – 3.5 ºC; Table 1) and higher oxygen concentration (Fig. S2a, S2b; Prieto et al. 2013; Dobal-Amador et al. 2016). Two types of intermediate waters were found, the Labrador Sea Water (LSW; 1800-2000 m) showed a minimum of salinity (35.0 – 35.4; Table 1) and a relatively high oxygen concentration (197.5 – 262.8 µmol kg^{-1}; Fig. S2a, S2b). The Mediterranean Water (MW; 1000 m depth) was clearly identifiable by the highest salinity values (35.0 - 36.2; Prieto et al. 2013; Table 1) as compared to the other water masses. The Eastern North Atlantic Central Water was found between 250 – 900 m depth and the Oxygen Minimum Zone (ENACW-OMZ) was located east of the Galician bank at around 900 m depth characterized by the lowest oxygen concentrations (180 – 241 mol kg^{-1}, Fig. S2a, S2b). The lowest concentrations of nitrate, phosphate and silicate (0.1 – 8.7, 0.1 – 0.7 and 0.2 – 4.4 µmol kg^{-1}, respectively) were found in the Euphotic Zone (EZ; 0-100 m depth).

Elemental and optical characterization of the DOM

The DOC concentration decreased from subsurface towards the deeper layers (Fig. 2a, 2b) with no significant differences between BIO-PROF-1 and BIO-PROF-2 cruises (t-test, $p=0.19$, $n=107$). The lowest DOC concentrations (42 – 44 µmol L^{-1}) were determined in the LDW. The

fluorescence of protein-like substances of the DOM showed significant differences between the two cruises (t-test, $p<0.01$, n=107), being lower during BIO-PROF-1. FDOM-T also decreased with depth, from 1.84 QSU at the EZ and reaching values of about 0.30 QSU in LDW (Fig. 2c, 2d). By contrast, the fluorescence of marine humic-like substances increased from ~0.60 QSU in EZ to 1.00 in LDW (Fig. 2e, 2f) and did not exhibit significant differences between the two cruises (t-test, p=0.13, n=107). None of the fluorescence indices showed any horizontal variability. The absorption coefficient at 254 nm (aCDOM254) (Fig. 3a, 3b) ranged from 1.32 at EZ to 0.84 at LDW with no significant differences between both cruises (t-test, p=0.52, n=107). On the other hand, aCDOM340 and aCDOM365 (Fig. 3c, 3d, 3e, 3f) did not show any vertical or horizontal trend with depth, presenting average values of 0.13 and 0.09, respectively. However, significant differences were found between both cruises (t-test, $p<0.01$, n=107), as both coefficients were higher in the shallower waters during BIO-PROF-2. The sCDOM275-295 decreased from 0.033 in the EZ to 0.027 in the LDW and significant differences were found between both cruises (t-test, $p<0.01$, n=54).

Prokaryotic abundance and leucine incorporation

The highest prokaryotic abundance (PA) occurred in the EZ ($2.33 \pm 0.8 \times 10^5$ cells mL^{-1}; Fig. 4a, 4b), decreasing exponentially with depth at all stations during both BIO-PROF-1 and BIO-PROF-2 cruises. No significant differences among PA distribution in the two cruises were observed (test?, p value?). The minimum values were found in the ENADW ($1.84 \pm 0.94 \times 10^4$ cells mL^{-1}; Fig. 4b) during BIO-PROF-2 cruise. The rates of leucine incorporation (Leu incorp.) showed a similar vertical trend at both cruises, decreasing three orders of magnitude from the EZ (7.85 ± 5 fmol Leu L^{-1} day^{-1}; Fig. 4c, 4d) to the LDW ($6.68 \pm 6.75 \times 10^{-3}$ fmol Leu L^{-1} day^{-1}; Fig. 4c, 4d). Cell-specific activity decreased from the euphotic zone to the intermediate and deep waters; however, it varied between cruises (Fig. 4e, 4f). Maximum cell-specific activity was $1.46 \pm 1.5 \times 10^{-5}$ fmol Leu $cell^{-1}$ day^{-1} in the EZ during the BIO-PROF-1 cruise (Fig. 4e). Generally, cell-specific activity was more variable in the intermediate and deep waters, particularly during the BIO-PROF-2 cruise, but always within one order of magnitude. In the intermediate and deep waters, the minimum cell-specific activity was $9.81 \pm 6.98 \times 10^{-6}$ fmol Leu $cell^{-1}day^{-1}$in the LDW during BIO-PROF-1, while the maximum was $1.13 \pm 1.04 \times 10^{-3}$fmol Leu $cell^{-1}$ day^{-1}in the EZ during BIO-PROF-2.

Microbial community structure determined by fingerprinting techniques

The terminal restriction fragment length polymorphism (T-RFLP) pattern of the archaeal community revealed a total of 133 OTUs at the 16S rRNA gene level, ranging from 46 to 918 bp. The T-RFLP fingerprints of specific water masses showed 106 OTUs in the EZ, 49 OTUs in

the ENACW-OMZ, 68 OTUs in the MW, 56 OTUs in the LSW, 67 OTUs in the ENADW and 26 OTUs in the LDW. The 14% of the 135 OTUs were present in all water masses, by contrast, 35% were unique to specific water masses. The archaeal community clustered according to different water masses (Fig. S3a): (i) the first cluster corresponded to archaeal communities inhabiting the euphotic zone (labelled in blue, Fig. S2a); (ii) the second set corresponded to archaeal communities in intermediate waters, ENACW-OMZ and MW (labelled in orange, Fig. S3a); and (iii) the third cluster corresponded to the deep waters, represented by LSW, ENADW and LDW (labelled in green, Fig. S3a).

On the other hand, the automated ribosomal intergenic spacer analysis (ARISA) patterns of the bacterial community revealed in total 290 different bacterial taxa (OTUs) on the internal transcribed spacer (ITS) region, ranging from 101 to 1017 bp. The ARISA profiles for the different water masses comprised 206 OTUs in the EZ, 172 OTUs in the ENACW-OMZ, 151 OTUs in the MW, 154 OTUs in the LSW, 169 OTUs in the ENADW and 124 OTUs in the LDW. The 16% of the 290 OTUs were present in all water masses, by contrast, 21% were unique to specific water masses. These specific OTUs led to a clear separation of bacterial communities according to three main groups of water masses: (i) one cluster comprised bacterial communities inhabiting in EZ (labeled in blue, Fig. S3b); (ii) the second cluster consisted of bacterial communities inhabiting the intermediate water masses, ENACW-OMZ and MW (labeled in orange, Fig. S3b); (iii) and the third cluster comprised the bacterial communities from the deep waters, comprised by LSW, ENADW and LDW (labeled in green, Fig. S3b).

Microbial community composition assessed by 454-pyrosequencing

A total of 29336 archaeal (on average 4191 sequences per sample, range 1436 – 8043) and 80659 bacterial (on average 13443 sequences per sample, range 3511 – 45269) sequences were obtained by 454 pyrosequencing from 7 samples, after quality check and denoising of the raw sequences. The total number of OTUs for Archaea and Bacteria was 275 and 1309 respectively. The highest richness (Chao1 richness index) of Archaea occured in ENACW-OMZ (141) decreasing towards the ENADW, which showed the minimum value (41, Table S2). Subsequently, the richness increased again at LDW (51). Similarly, Bacteria also revealed a maximum of Chao1 index richness in the ENACW-OMZ (638) and decreased towards deep reaching the minimum in the LDW (222, Table S2).

The taxonomy of Archaea (Fig. 5a) and Bacteria (Fig. 5b) was studied at the order and family level. The archaeal community was composed by the phyla Euryarchaeota and Thaumarchaeota contributing 17 and 83% to the total archaeal 16S rRNA gene sequences, respectively. Euryarchaeota was dominated by Thermoplasmata, mainly by the Marine Group II (MGII) with

an average relative abundance among all water masses of 14%, and relative abundances up to 40% in the ENACW-OMZ and in the LSW. Additionally, on average 3% of the sequences were identified as Marine Group III (MGIII). The most abundant order of Thaumarchaeota was Marine Group I (MGI 81%) with the maximum relative abundance located in the EZ and in the MW (Fig. 5a).

The bacterial community showed a larger number of different phyla compared to Archaea (Fig. 5b). Taking into account the whole Bacteria dataset, we found that most sequences belonged to the phyla Proteobacteria (80%). The most abundant classes of Proteobacteria were the Alphaproteobacteria (56%) with the highest abundance found in the EZ (82%). Delta- and Gammaproteobacteria made up to 14 and 8% of total Bacteria, respectively. Delta- accounted for 24% of total Proteobacteria in the LSW, while Gammaproteobacteria showed the highest abundance located in the LDW (36% of total Proteobacteria). Interestingly, Vibrionaceae accounted for 3.5% of total bacterial sequences, however, 24.3% of Vibrionaceae sequences were found in the LDW. Cyanobacteria sequences, belonging to Prochlorococcus, were on average 6% of the total bacterial community, and showed the maximum relative abundance in the ENACW-OMZ. Additionally, SAR202 (4%) was the dominant group within the Chloroflexi class, with maxima relative abundance in the ENADW and in the LDW. Other less abundant groups were Bacteroidetes (3%), Actinobacteria (2%), Deferribacteres (1%) and Planctomycetes (1%). Despite the majority of the samples were dominated by Proteobacteria, differences between the different water masses were observed at lower phylogenetic levels.

Flavobacteriaceae was present in the ENACW-OMZ (3%; Fig. 5b). Within Alphaproteobacteria, we found three members of SAR11 at family level (SAR11clade, SAR11 surface and SAR11 deep). SAR11clade and SAR11 surface were more abundant in the EZ and in the ENACW-OMZ (Fig. 5b) as compared to SAR11 deep or SAR11clade. However, SAR11 deep showed the highest relative abundance in the LSW (Fig. 5b). Rhodospirillaceae had higher relative abundance in the MW and in the LSW than Ricketssiales, which peaked in the ENADW and in the LDW (Fig. 5b). Nitrospinaceae, the second most abundant group of Deltaproteobacteria, was relatively more abundant in the EZ and in the MW (Fig. 5b) than in deep waters. Within Gammaproteobacteria, the most frequent phylotypes at family level were Colwellia, JL-ETNP-Y6 (Oceanospirilla), Oceanospirillaceae and Vibrionaceae. These phylotypes showed their maximum relative abundance in the LDW (Fig. 5b). The relative abundance of Mariprofundaceae (Zetaproteobacteria) ranged between 0.1 – 1% of total bacteria, with maximum values located in the MW and in the ENADW.

Bacterial and archaeal abundance assessed by CARD-FISH

449 The contribution of Bacteria to the total prokaryotic community decreased from the euphotic
450 zone (~60%) to the deep waters (~45%) (Table 2). By contrast, the relative abundance of
451 Thaumarchaeota (% of DAPI, Table 2) tended to increase with depth. The highest relative
452 abundance was found in the oxygen minimum zone and deep waters, however, Thaumarchaeota
453 never reached values higher than ~15%. The abundance of both, Thaumarchaeota and Bacteria,
454 did not show significant differences among BIO-PROF-1 and BIO-PROF-2 (t-test, $p>0.05$,
455 n=22).
456
457 **DOM variables influencing the microbial communities**
458 Marginal test were calculated to explain the contribution of each DOM-variable separately on
459 the archaeal community structure using T-RFLP fingerprinting and bacterial community
460 structure using ARISA fingerprinting results. DOC, FDOM-T, FDOM-M, aCDOM254,
461 sCDOM275-295 and depth were significantly related with the archaeal community composition
462 (Table S3). FDOM-M and FDOM-T were the main explanatory factors identified by DistLM of
463 the archaeal community structure (Table 3) for the whole dataset (n=48), explaining together
464 18% of the total variability. However, different depth layers showed different predictor
465 variables. The main predictor factor for the variability in archaeal community structure in the
466 euphotic zone (n=11) was aCDOM254, explaining 22.3% of the total variation. Alternatively,
467 FDOM-T, aCDOM254, depth, sCDOM275-295, DOC and FDOM-M explained most of the
468 variability in archaeal community structure in the intermediate waters (54.4%, n=19). In the
469 deep waters (n=18), FDOM-M was the only significant variable, accounting for 11.7% of the
470 variation in archaeal community structure (Table 3).
471 Similarly, the marginal test for bacterial communities revealed significant effects of DOC,
472 FDOM-T, FDOM-M, sCDOM275-295 and depth (Table S4). Considering the whole water
473 column (n=63), the DistLM sequential test showed that FDOM-M, depth, aCDOM365,
474 aCDOM340, FDOM-T and sCDOM275-295 were related with the bacterial community
475 composition, explaining 36% of the total variation (Table 4). However, depth was the only
476 variable that significantly explained the variation in the bacterial community structure from the
477 euphotic zone (13.2%; n=18). sCDOM275-295, depth and aCDOM340 accounted for 29.2%,
478 12.1% and 5.7% of the total variation in bacterial community structure from the intermediate
479 waters (n=25). The main predictor factors for the variability in bacterial community from the
480 deep waters (n= 20) were the aCDOM365, depth and sCDOM275-295, with 7.9%, 11.1% and
481 12.6%, respectively (Table 4).
482 Redundancy analysis (RDA) was performed to examine how DOM-variables were associated to
483 specific microbial 454-pyrosequencing phylotypes (Fig. 6). Microbial phylotypes in the

different water masses were associated to different DOM-variables. Axes 1 and 2 were interpreted as (i) depth/DOM quantity and (ii) DOM quality, respectively.
The FDOM-M showed positive correlation with both axes. Depth presented a positive correlation with axis 1 and negative correlation with axis 2. sCDOM275-295 , aCDOM365, aCDOM340, aCDOM354 and FDOM-T displayed a negative correlation with axis 1 and positive with axis 2. In addition, Euryarchaeota-MGIII, which had its highest relative abundance in ENADW, was significantly associated to FDOM-M. Furthermore, sCDOM275-295 was connected to Thaumarchaeota-MGI and also to the bacterial groups Acidobacteria and SAR324 clade. Flavobacteria and OCS116 clade were related to aCDOM365. RDA also suggests a strong link between aCDOM254 and bacterial members inhabiting ENACW-OMZ, i.e. SAR11 clade, Rhodobacterales, SAR116 clade and Verrucomicrobia. Additionally, the DOC concentrations were correlated with the relative abundance of Nitrospirillaceae. By contrast, the increasing relative abundance of SAR202 clade, SAR406 clade, SAR286 clade, Rickettsiales and Rhizobiales with depth were related to FDOM-M.

DISCUSSION

Archaeal and Bacterial communities inhabiting the euphotic, intermediate and deep waters has been described for the first time in the euphotic and dark waters off the Galician coast. The microbial abundance, activity and community composition showed clear vertical trends consistent with the vertical stratification of environmental and optical characterization of DOM. DOM variables presented higher concentrations at the surface that decreased with depth, except for FDOM-M that increases with depth, showing the highest values at the deeper layers, as described previously (Carlson and Hansell 2015; Stedmon and Nelson 2015). Globally, all the DOM values were consistent with previous measurements in this region (Lønborg and Alvarez-Salgado, 2014). Correspondingly, the highest abundance and leucine incorporation of the prokaryotic communities was found in the euphotic zone, characterized by a highest temperature, oxygen and organic matter bioavailability that facilitate the growth of microbes. On the other hand, the abundance and activity decreases with increasing depth by 2 and 3 orders of magnitude, respectively, and environmental conditions may only allow the growth of specific microbes associated to dark waters.

Vertical distribution of specific archaeal and bacterial phylotypes

Vertical microbial distribution patterns suggest habitat partitioning, where Bacteria is dominant at the surface waters and Archaea is more abundant in OMZ and deeper waters, as previously reported for other regions of the North Atlantic ocean (Herndl et al. 2005; Teira et al. 2006; Varela et al. 2008b; Agogué et al. 2011).

Thaumarchaeota dominated over Euryarchaeota and exhibited a patchy vertical distribution. The high abundance of Thaumarchaeota-MGI found in the EZ and in the ENADW waters have also been observed in previous studies (Herndl et al. 2005; Teira et al. 2006; Varela et al. 2008b). Ferrera et al. (2015) found all Euryarchaeota related to the class Thermoplasmata in northeastern Atlantic Ocean in agreement with our results off the Galician coast. The Euryarchaeota-MGII vertical distribution, with maximum relative abundance in OMZ, indicates an adaptation of members of this group to low oxygen concentrations. The highest abundance of Thaumarchaeota in this area is found in layers with lower oxygen concentrations as compared to surface and deep waters, in agreement with previous studies in ocean ecosystems (Francis et al. 2005; Lam et al. 2007). These decreased oxygen layers are suitable to harbour redox processes, such as ammonia oxidization (Zehr and Ward, 2002; Konneke et al. 2005; Sintes et al. 2013) and, consequently, the organisms inhabiting them can potentially exhibit authotrophic metabolism (Guerrero-Feijoo et al. personnel communication). However, Thaumarchaeota also showed high relative abundance in the euphotic zone and the deeper layers linked to the highest DOC concentration, suggesting mixotrophic metabolism and different substrate preferences for different Thaumarchaeota ecotypes (Sintes et al. 2016; Smith et al. 2016).

Our results support that members of the SAR11 clade of Alphaproteobacteria are the most abundant and ubiquitous bacterial organisms in the ocean, indicating high competition for available resources, particularly in the ocean surface (Giovanni and Rappé, 2000; Morris et al. 2002; DeLong et al. 2006; Dobal-Amador et al. 2016). By contrast, the Gammaproteobacteria were the dominant group in the deeper waters, particularly in the LDW, in accordance with current knowledge of bacterial communities from marine ecosystems (Lopez-Garcia et al. 2001; Sogin et al. 2006; Lauro and Bartlett, 2008). Alteromonas identified by 16S rRNA gene 454sequences showed a patchy distribution as compared to CARD-FISH counts from the same cruise which showed a decreasing relative abundance with depth (Doval-Amador et al. 2016). Both 454 pyrosequencing of these study and CARD-FISH counts (Doval-Amador et al. 2016) methods showed a clear increasing trend of SAR324 clade with depth (maximum relative abundance was located in the LSW). The enrichment of this group could reflect an important role of the chemoautotrophic metabolism in the deep water masses, since previous studies based on single cell genomic analyses have shown that members of the SAR324 clade contain sulphur oxydizing genes in the intermediate and deep waters and are capable of inorganic carbon fixation (Swan et al. 2011; Sheik et al. 2014).

SAR202 clade has been described as a deep bacterial phylotype in the deep north Atlantic waters (Varela et al. 2008b) and an r-strategist, which can rapidly exploit nutrient patches in the dark ocean (Varela et al. 2008b). Another prominent group in deep waters off the Galician coast

555 was SAR406 clade, in agreement with previous reports (Gordon and Giovannoni, 1996;
556 Gallagher et al. 2004; Pham et al. 2008; Galand et al. 2010). SAR406 members contain
557 inorganic sulfur metabolic pathways (Yamamoto and Takai, 2011), suggesting a possible role of
558 these organisms as sulfate-reducers. Bacteroidetes is more abundant in surface than deep waters
559 (Chauhan et al. 2009), in agreement with their ability to use high molecular weight DOM
560 biopolymers (Kirchman, 2001).

561 Although a correlation between the results obtained by the CARD-FISH analysis (Doval-
562 Amador et al. 2016) and the 16S rRNA gene amplicon 454-pyrosequencing could not be
563 performed as these different techniques target different 16S gene regions, we found a good
564 correspondence between the vertical distributions of the specific groups of Bacteria by both
565 methodologies. The contribution of SAR324 and SAR406 to the bacterial community as
566 determined by CARD-FISH and pyrosequencing was close to the 1:1 line (data not shown),
567 indicating that both techniques retrieved this cluster with similar efficiency. By contrast, the
568 relative abundance of SAR11 was higher in the pyrosequencing dataset than with CARD-FISH
569 (data not shown, t-test, $p<0.05$). Alteromonas and SAR202 contributed disproportionally more
570 to bacterial abundance using CARD-FISH than using pyrosecuencing (data not shown, t-test,
571 $p<0.05$). These different patterns could be explained either by the different number of samples
572 analysed with the two methodologies or due to the PCR-bias associated to the pyrosequencing
573 approach as compared to CARD-FISH, where the probes target directly the 16S rRNA.
574
575 **Importance of DOM-related variables influencing the microbial community structure and**
576 **composition**
577 Microbial community composition correlates with a variety of abiotic parameters (such as
578 temperature and salinity) of the water masses (Yokokawa et al. 2010; Agogué et al. 2011;
579 Sjöstedt et al. 2014; Dobal-Amador et al. 2016). Moreover, microbial community composition
580 varies according to DOM composition (Kirchman et al. 2004). Several studies have found that
581 the microbial production of recalcitrant DOM (mostly humic substances) as a sub-product of the
582 remineralisation processes adds up complexity to this relationship (Jiao et al. 2010; Nieto-Cid et
583 al. 2006). Standard physico-chemical variables were the main factor explaining the variability of
584 the bacterial community vertical distribution in the deep waters of the Galician coast (Doval-
585 Amador et al., 2016). However, in this previous study it was also indicated that some optical
586 DOM characteristics further explain the variability in the bacterial community structure through
587 the water column (Doval-Amador et al. 2016). Nevertheless, our knowledge on the DOM
588 composition and the link between microbial communities and the DOM acting as substrate/sub-
589 product of bacterial and archaeal metabolism in the deep ocean remains enigmatic. Both labile

and refractory compounds, represented by FDOM-T and FDOM-M, respectively, related differently with the microbial communities off the Galician coast. Whereas, the archaeal communities from the intermediate layers are linked to more labile molecules (protein-like material), which could be preferentially respired by these organisms, the archaeal communities of the deep waters are related to more refractory compounds. The strong positive correlation among FDOM-M and the relative abundance of Archaea, particularly Euryarchaeota-MGII, support the concept of the microbial carbon pump (MCP; Jiao et al. 2010), as these deep-ocean microbial communities are more connected to the refractory DOM (humic-like compounds) generated by themselves as sub-products of their respiratory metabolism.

Variations in bacterial community structure of the samples from the EZ are associated with depth, which is probably related to temperature and other physical parameters (Yokokawa et al. 2010, Sjöstedt et al. 2014), as well as chlorophyll a and the DOM availability (Walsh et al. 2015). The sCDOM275-295 was the main explanatory DOM-related variable for bacterial community structure in the intermediate and deep waters, suggesting a tight coupling between the bacteria and the aromaticity and molecular weight of the DOM (Helms et al. 2008). This finding would indicate that the molecular weight of the DOM, very likely associated to DOM ageing in the water masses (Helms et al. 2008), is linked to the changes in the bacterial community structure within the dark ocean. The strong relationship of Acidobacteria and SAR324 clade, typical deep-sea groups, with sCDOM275-295, suggests a higher contribution of these organisms to transform DOM into older, bigger and more aromatic compounds. Furthermore, the relationship of bacterial communities from intermediate waters with aCDOM340 (mainly Nitrospirae) and the relationship of the bacterial communities inhabiting the deeper layers with aCDOM365 (Mariprofundaceae and Gemmatimonadetes) suggest that the deep water bacterial communities metabolize DOM with a higher degree of aromaticity (more refractory) than the bacterial communities of the intermediate waters (absorption wavelength of 365 nm versus 340 nm; Stedmon & Nelson 2015). The relationships between DOM variables and the distribution patterns of Flavobacteria, Myxococcales, SAR11 clade, SAR86 clade, SAR116 clade, SAR202 clade, SAR324 clade, SAR406 clade, Rhodobacteraceae, Rickettsiales, Planctomycetes and Verrucomicrobia, support the notion of a heterotrophic (or mixotrophic) lifestyle of these groups. Flavobacteria (Bacteroidetes) and SAR86 (Gammaproteobacteria) have been reported before as important players in DOM cycling, especially from the high molecular weight fraction of DOM (Kirchman et al. 2002; Nikard et al. 2014). Nevertheless, several bacterial groups, such as SAR202 clade (Chloroflexi), SAR406 clade (Deferribacteres), Rickettsiales (Alphaproteobacteria) and Rhizobiales (Alphaproteobacteria), showed also a strong correlation with FDOM-M indicative of their potential to generate refractory compounds of DOM (humic-like compounds), as sub-products of the remineralization processes.

Our data suggest that both archaeal and bacterial communities are coupled to compositional changes in the DOM pool. The increasing/decreasing patterns of FDOM-M and FDOM-T with depth are the main variables related to the vertical stratification of microbial communities, however, the absorption coefficients at 254, 340 and 365 nm are also affected by the stratification of microbial communities in the eastern north Atlantic ocean. Some phylotypes, such as SAR202 and SAR406 might be able to relate to both labile and refractory-DOM, while others, such as Thaumarchaeota-MGI, display preferential relations with aromatic compounds in the deep waters.

ACKNOWLEDGEMENTS

We thank the Captain and the Crew of R/V Coornide de Saavedra for their support during the BIO-PROF-1 and BIO-PROF-2 cruises. We thank F. Eiroa for assistance with onboard and flow cytomety measurements, C. Carballo helped with the inorganic nutrient analysis. X.A. Álvarez-Salgado, M.J. Pazó and J. Pampín for support with the chemical characterization. E. Teira and G.J. Herndl for their support with the fingerprinting analysis and J.M. Gasol with pyrosequencing bioinformatic analysis. High-Performance computing analyses were run at the Marine Bioinformatics Service of the Institut de Ciències del Mar (ICM-CSIC) in Barcelona. Funding for the sampling and analysis was supported by the projects “Biodiversidade Funcional do Microplancton nas profundidades mariñas de Galicia” (BIO-PROF, Ref. 10MMA604024PR, 2010-2012, Xunta de Galicia) and “Fuentes de Materia Orgánica y Diversidad Funcional del Microplancton en las aguas profundas del Atlántico Norte” (MODUPLAN, Plan Nacional I+D+I) to MMV. MNC was funded by the CSIC Program “Junta para la Ampliación de Estudios” co-financed by the ESF (reference JAE DOC 040) and the project FERMIO (MINECO, CTM2014-57334-JIN). EGF was supported by the BIO-PROF and MODUPLAN projects. VHM was supported by the MICINN program “Formación de Personal Investigador” (FPI), Ref. grant BES-2009-028186. ES was supported by the Austrian Science Fund (FWF) project P27696-B22. This work is in partial fulfillment of the requeriments for a Ph.D. degree from the Universidade de A Coruña by E.G.-F.

655 **REFERENCES**

656 Agogué H, Lamy D, Neal PR, et al. Water mass-specificity of bacterial communities in the
657 North Atlantic revealed by massively parallel sequencing. *Mol Ecol* 2011;**20**: 258-278.

658 Álvarez-Salgado XA, Miller AEJ. Simultaneous determination of dissolved organic carbon and
659 total dissolved nitrogen in seawater by high temperature catalytic oxidation: conditions
660 for precise shipboard measurements. *Mar Chem* 1998;**62:** 325–333.

661 Anderson M.J. A new method for non-parametric multivariate analysis of variance, *Austral.*
662 *Ecol* 2001;**26:** 32–46.

663 Anderson MJ, Gorley RN, Clarke KR. PERMANOVA+ for PRIMER: Guide to Software and
664 Statistical Methods 2008. PRIMER-E, Plymouth, UK.

665 Arístegui J, Gasol JM, Duarte CM, et al. Microbial oceanography of the dark ocean's pelagic
666 realm. *Limnol Oceanogr* 2009;**54**: 1501-1529.

667 Caporaso JG, Kuczynski J, Stombaugh J, et al. QIIME allows analysis of high-throughput
668 community sequencing data. *Nat Methods* 2010;7: 335-336.

669 Cardinale M, Brusetti L, Quatrini P, et al. Comparison of different primer sets for use in
670 automated ribosomal intergenic spacer analysis of complex bacterial communities. *Appl*
671 *Environ Microbiol* 2004;**70:** 6147-6156.

672 Carlson CA, Hansell DA. 2015 "DOM sources, sinks, reactivity, and budgets". In
673 Biogeochemistry of Marine Dissolved Organic Matter, Hansell & Carlson, 2015.
674 doi.org/10.1016/B978-0-12-405940-5.00010-8. Elsevier Inc.

675 Chauhan A, Cherrier J, Williams, HN. Impact of sideways and bottom-up control factors on
676 bacterial community succession over a tidal cycle. *Proc Natl Acad Sci USA* 2009;**106**:
677 4301-4306.

678 Cottrell MT, Kirchman DL. Community composition of marine bacterioplankton determinate
679 by 16S rRNA gene clone libraries and fluorescence in situ hybridization. *Am. Soc.*
680 *Microbiol.* 2000;**66:** 5116-5122.

681 DeLong EF. Archaea in coastal marine environments. *Proc Natl Acad Sci USA* 1992;**89**: 5685-
682 5689.

683 DeLong EF, Preston CM, Mincer et al. Community genomics among stratified microbial
684 assemblages in the ocean's interior. *Science* 2006;**311:** 496-503.

685 Dobal-Amador V, Nieto-Cid M, Guerrero-Feijóo E, et al. Vertical patterns of bacterial
686 abundance, activity and community composition in the dark waters of the Galician coast
687 (NW Spain). 2016. *Deep-Sea Res Part I* 114:1-11.

688 Ferrera I, Arístegui J, Gonzalez JM, et al. (2015) Transcient Changes in Bacterioplankton
689 Communities Induced by the Submarine Volcanic Eruption of El Hierro (Canary Islands).
690 *PLoS ONE* 2015, DOI: 10.1371/journal.pone.0118136.

691 Francis CA, Roberts KJ, Beman JM, et al. Ubiquity and diversity of ammonia-oxidizing archaea
692 in water columns and sediments of the ocean. *Proc Natl Acad Sci USA* **2005;102:**14683–
693 14688.
694 Frank AH, Garcia JA, Herndl GJ, Reinthaler T. Connectivity between surface and deep waters
695 determines prokaryotic diversity in the North Atlantic Deep Water. *Environ Microbiol*
696 2016, DOI: 10.1111/1462-2920.13237
697 Furhman JA, Steele JA, Hewson et al. A latitudinal diversity gradient in planktonic marine
698 bacteria. *Proc Natl Acad Sci* USA 2008; 105; 7774-7778.
699 Furhman JA, Cram JA, Needham DM. Marine microbial community dynamics and their
700 ecological interpretation. *Nat Rev Microbiol* 2015;**13**: 133-146.
701 Galand PE, Lovejoy C, Amilton AK, et al. Archaeal diversity and gene for ammonia oxidation
702 are coupled to ocean circulation. *Environ Microb* 2010;**11:** 971-980.
703 Gallagher JM, Carton MW, Eardly DF, Patching JW. Spatio-temporal variability and diversity
704 of water column prokaryotic communities in the eastern North Atlantic. *FEMS Microbiol*
705 *Ecol* 2004;**47:**249-262.
706 García-Martinez J, Acinas SG, Anton AI, Rodriguez-Valera F. Use of the 16S--23S ribosomal
707 genes spacer region in studies of prokaryotic diversity. *J Microbiol Methods* 1999;**36**:55-
708 64
709 Gasol JM, Zweifel U, Peters F, et al. Significance of Size and Nucleic Acid Content
710 Heterogeneity as Mesured by Flow Cytometry in Natural Planktonic Bacteria. Appl
711 *Environ Microbiol* 1999;**65**: 104475-104483.
712 Giovannoni SJ, Rappe MS, Vergin, KL, Adair NL. 16S rRNA genes reveal stratified open
713 ocean bacterioplankton populations related to the green non-sulfur bacteria. *Pro Natl*
714 *Acad Sci USA* 1996;**93:** 7979-7984.
715 Giovannoni S, Rappé M. Evolution, diversity, and molecular ecology of marine prokaryotes.
716 Microbial Ecology of the Oceans, 1st ed (Kirchman, D. L, ed), pp. 47-84. John Wiley and
717 Sons, Inc, New York, 2000.
718 Gordon DA, Giovannoni SJ. Detection of stratified microbial populations related to Chlorobium
719 and Fibrobacter species in the Atlantic and Pacific Oceans. *Appl Environ Microbiol*
720 1996;**4:**1171-1177.
721 Green SA, Blough NV. Optical absorption and fluorescence properties of chromophoric
722 dissolved organic matter in natural waters, *Limnol Oceangr* 1994;**29:** 1903-1916.
723 Guerrero-Feijóo E, Nieto-Cid M, Sintes E, Varela MM. Bacterial activity and community
724 composition response to the size-reactivity of disolved organic matter. 2015. Personnel
725 communication. SAME14 Second EMBO Conference. Uppsala. Sweeden.

Haas BJ, Gevers D, Earl AM, Feldgarden M, et al. Chimeric 16S rRNA sequence for mation and detection in Sanger and 454-pyrosequenced PCR amplicons. *Genome Res* 2011;**21:** 494-504.

Hansen HP, Koroleff F. Determination of nutrients. In: Grasshoff K, Kremling, K, Ehrhardt, M. (ed), Methods of Seawater Analysis, 3rd edition Wiley-VCH Verlag GmbH: 1999.

Helms JR, Stubbins A, Ritchie JD, et al. Absorption spectral slopes and slope ratios as indicators of molecular weight, source and photobleaching of chromophoric dissolved organic matter. *Limnol Oceanogr* 2008;**51:** 2170-2180.

Herndl GJ, Reinthaler T, Teira E, et al. Contribution of Archaea to total prokaryotic production in the deep Atlantic Ocean. *Appl Environ Microbiol* 2005;**71:** 2303-2309.

Hewson I, Furhman JA. Spatial and vertical biogeography of coral reef sediment bacterial and diazotroph communities. Mar Ecol Prog Ser 2006; 306: 79-86.

Jiao N, Herndl GJ, Hansell,DA, et al. Microbial production of recalcitrant dissolved organic matter: long-term carbon storage in the global ocean. *Nat Rev Microb* 2010;**8:** 593-599.

Karner MB, DeLong EF, Karl DM. Archaeal dominance in the mesopelagic of the Pacific Ocean. *Nature* 2001;**409:** 507-510.

Kirchman DL. Measuring bacterial biomass production and growth rates from leucine incorporation in natural aquatic environments. In: Paul JH (ed) *Methods in microbiologoy*, Academic Press, 2001, 227-237.

Kirchman DL. The ecology of Cytophaga-Flavobacteria in aquatic environments. FEMS *Microbiol Ecol* 2002;**39**: 91-100.

Kirchman DL, Dittel AI, Findlay, SEG, Fische D. Changes in bacterial activity and community structure in response to organic matter in the Hudson River, New York. *Aquat Microb Ecol* 2004;**34**: 243-257.

Kirchman DL, Knees E, Hodson R. Leucine incorporation and its potential as measure of protein synthesis by bacteria in natural aquatic system. *Appl Environ Microbiol* 1985;**49**: 599-607.

Könneke MB, DeLong EF, Karl DM. Isolation of an autotrophic ammonia-oxidizing marine archaeon. *Nature* 2005;**437:** 543-546.

Lam P, Jensen MM, Lavik G, et al. Linking crenarchaeal and bacterial nitrification to anammox in the Black Sea. *Proc Natl Acad Sci USA* 2007;**104:** 7104-7109.

Langdon C. Determination of dissolved oxygen in seawater by winkler titration using the amperometric technique. IOCCP Report Nº 14, ICPO publication series N 134. 2010.

Lauro FM, Bartlett DH. Prokaryotic lifestyles in deep sea habitats. *Extremohiles* 2008;**12:** 15-25.

761 Lekunberri I, Sintes E, DeCorte D, Yokokawa T, Herndl GJ. Spatial patterns of bacterial and
762 archaeal communities along the Romanche Fracture Zone. *FEMS Microbiol Ecol*
763 2016;**85:** 537-552.
764 Leuko S, Goh F, Ibáñez-Peral R, Burns BP, Walter MR, Neilan BA. Lysis efficiency of
765 standard DNA extraction methods for Halococcus spp. in an organic rich environment.
766 *Extremophiles* 2008;**12**:301-8.

767 Lopez-Garcia P, Lopez-Lopez A, Moreira D, Rodriguez-Valera F. Diversity of free-living
768 prokaryotes from a deep-sea site at the Antarctic Polar Front. *FEMS Microbiol Ecol*
769 2001;**36**: 193-202.
770 Martín-Cuadrado AB, López-García P, Alba JC, et al. Metagenomics of the Deep
771 Mediterranean, a Warm Bathypelagic Habitat. *PloS ONE* 2007;2(9): e914.
772 Moesender MM, Winter C, Arrieta JM, Herndl GJ. Terminal-restriction fragment length
773 polymorphism (T-RFLP) screening of a marine archaeal clone library to determine the
774 different phylotypes. *J Microbiol Methods* 2001;44: 159-172.
775 Moreira D, Rodríguez-Varela F, López-García P. Analysis of a genome fragment of a deep-sea
776 uncultivated Group II euryarchaeote containing 16S rDNA, a spectinomycin-like operon
777 and several energy metabolism genes. *Environ Microbial* 2004;**6**: 959–969
778 Morris RM, Rappé MS, Connon SA, et al. SAR11 clade dominates ocean surface
779 bacterioplankton communities. *Nature* 2002;420: 806-810.
780 Nieto-Cid M, Alvarez-Salgado XA, Perez FF. Microbial and photochemical reactivity of
781 fluorescent dissolved organic matter in a coastal upwelling system. *Limnol Oceanogr*
782 2006;**51:** 1391-1400.
783 Nikard MP, Cottrell MT, Kirchman DL. Uptake of dissolved organic carbon by
784 gammaproteobacterial subgroups in coastal waters of the West Antarctic Peninsula. *Appl*
785 *Environ Microbiol* 2014;**80:** 3362-3368.
786 Pernthaler A, Pernthaler J, Amann R. Fluorescence in situ hybridization and catalyzed reported
787 deposition for the identification of marine bacteria. *Appl Environ Microbiol* 2002;**68:**
788 3094-3101.
789 Pham VD, Konstantinidis KT, Palden T, DeLong EF. Phylogenetic analyses of ribosomal DNA-
790 containing bacterioplankton genome fragments from a 4000 m vertical profile in the
791 North Pacific Subtropical Gyre. *Environ Microbiol* 2008;10: 2313-2330.
792 Prieto E, González-Pola C, Lavín S, et al. Seasonality of intermédiate waters hydrography west
793 of the Iberian Peninsula from an 8 year semiannual time series of an oceanographic
794 section. *Ocean Sci* 2013;**9:** 411-429.

795 Reeder J, Knight R. Rapidly denoising pyrosequencing amplicon reads by exploiting rank-
796 abundance distributions. *Nat Methods* 2010;**7**: 668 – 669.
797 Schloss PD, Westcott SL, Ryabin T, et al. Introducing MOTHUR: Open-source, platform-
798 independent, community-supported software for describing and comparing microbial
799 communities. *Appl Environ Microbiol* 2009;**75**: 7537-7541.
800 Schmidt TM, DeLong EF, Prace NR. Analysis of a marine picoplankton community by 16S
801 rRNA gene cloning and sequencing. *J Bacteriol* 1991;**173:** 4371-4378.
802 Sheik CS, Jain S, Dick GJ. Metabolic flexibility of enigmatic SAR324 revealed through
803 metagenomics and metatranscriptomics. *Environ Microbiol* 2014;**16:** 304–317.
804 Simon M, Azam F. Protein content and protein synthesis rates of planktonic marine bacteria.
805 *Mar Ecol Progr Ser* 1989;**51**: 201–13.
806 Sintes E, Bergauer K, De Corte D, et al. Archaeal amoA gene diversity points to distintic
807 biogeography of ammonia-oxidizing Crenarchaeota in the ocean. *Environ Microbiol*
808 2013;**15:** 1647-1658.
809 Sintes E, De Corte D, Haberleitner E, Herndl GJ. Geographic Distribution of Archaeal
810 Ammonia Oxidizing Ecotypes in the Atlantic Ocean. *Front Microbiol* 2016, doi:
811 10.3389/fmicb.2016.00077.
812 Sjöstedt J, Martiny JBH, Munk P, Riemann L. Abundance of broad bacterial taxa in the
813 Sargasso Sea Explained by environmental conditions but not water mass. *App Environ*
814 *Microbiol* 2014;**80:** 2786-2794
815 Smith DC, Azam F. A simple, economical method for measuring bacterial protein synthesis
816 rates in seawater using 3 H-leucine. *Mar Microb Food Webs* 1992;**6**: 107–114.
817 Smith JM, Damashek J, Chavez FP, Francis CA. Factors influencing nitrification rates and the
818 abundance and transcriptional activity of ammonia-oxidizing microorganisms in the dark
819 northeast Pacific Ocean. *Limnol Oceanogr 2016,* doi: 10.1002/lno.10235. [Epub ahead of
820 print].
821 Sogin ML, Morrison HG, Huber JA, et al. Microbial diversity in the deep sea and the
822 underexploresd 'rare biosphere'. *Proc Natl Acad Sci USA* 2006;**103:** 12115-12120.
823 Stedmon CA, Nelson NB. 2015 "The optical properties of DOM in the ocean". In
824 Biogeochemistry of Marine Dissolved Organic Matter, Hansell & Carlson, 2015.
825 doi.org/10.1016/B978-0-12-405940-5.00010-8. Elsevier Inc.
826 Swan BK, Martinez-Garcia M, Preston CM. Potential for chemolithoautotrophy among
827 ubiquitous bacteria lineages in the dark ocean. *Science* 2011;**333:** 1296-1300.
828 Teira E, Lebaron P, van Aken H, Herndl GJ. Distribution and activity of Bacteria and Archaea
829 in the deep waters masses of the North Atlantic. *Limnol Oceanogr* 2006a;**54:** 2131-2144.

Varela M, van Aken H, Herndl GJ. Abundance and activity of Cloroflexi-type SAR202 bacterioplankton in the meso- and bathypelagic waters of the (sub)tropical Atlantic. *Environ Microbiol* 2008a;**10:** 1903-1911.

Varela M, van Aken H, Sintes,E, Herndl GJ. Latitudinal trends of Crenarchaeota and Bacteria in the meso- and bathypelagic waters of the eastern north Atlantic. *Environ Microbiol* 2008b;**10:** 110-124.

Walsh E, Smith D, Sogin M, D'Hondt S. Bacterial and archaeal biogeography of the deep chlorophyll maximum in the South Pacific Gyre. *Aquat Microb Ecol* 2015;**75:** 1-13.

Wang Q, Garrity GM, Tiedje JM, Cole JR. (2007) Naieve Bayesian classifier for rapid assignment of rRNA sequences into the new bacterial taxonomy. *Appl Enviro Microbio* 2007;**73:** 5261 – 5267.

Winter C, Moeseneder MM, Herndl GJ, Weinbauer MG. Relationship of Geographic Distance, Depth, Temperature, and Viruses with Prokaryotic Communities in the Eastern Tropical Atlantic. *Microb Ecol* 2008; 56: 383-389.

Yamamoto M, Takai K. Sulfur metabolisms in epsilon- and gamma-Proteobacteria in deep-sea hydrothermal fields. *Front Microbiol* 2011;**2:** 1-8.

Yokokawa T, DeCorte D, Sintes E, Herndl, GJ. Spatial patterns of bacterial abundance, activity and community composition in relation to wáter masses in the Eastern Mediterrean Sea. *Aquat Microbiol Ecol* 2010;**59:** 185-195.

Zehr JP, Ward BB. Nitrogen cycling in the ocean: new perspectives on processes and paradigms. *Appl Environ Microbiol* 2002;**68:**1015-1024.

FIGURE LEGENDS:

Figure 1. Map showing the stations along the Finisterre Section located in the NW Atlantic Ocean off the Galician coast. Dots represent the stations where the physico-chemical data were measured. The stations where the biological measurements were conducted are also indicated (St11, St16, St108 and St 111).

Figure 2. Potential temperature (Tpot, ºC) - salinity diagrams every 2 dbars for the BIO-PROF-1 (Left) and BIO-PROF-2 (Right), with superimposed values from discrete depths of: (a, b) DOC in µmol kg^{-1}; (c, d) protein-like fluorescence, FDOM-T; (e, f) humic-like fluorescence, FDOM-M.

Figure 3. Potential temperature (Tpot, ºC) - salinity diagrams every 2 dbars for the BIO-PROF-1 (Left) and BIO-PROF-2 (Right), with superimposed values from discrete depths of: (a, b) absorption coefficient at 254 nm, (c, d) absorption coefficient at 365 nm and (e, f) optical slope between 275 and 295 nm.

Figure 4. Potential temperature (Tpot, ºC) - salinity diagrams every 2 dbars for the BIO-PROF-1 (Left) and BIO-PROF-2 (Right), with superimposed values from discrete depths of: (a, b) prokaryotic abundance (10^5 cells mL^{-1}); (c, d) leucine incorporation rate (pmol Leu L^{-1} h^{-1}); (e, f) cell-specific activity (10^{-4} pmol Leu $cell^{-1}$ h^{-1}).

Figure 5. Taxonomic classification of (a) archaeal and (b) bacterial sequences retrieved from different water masses at the family level from 16S rRNA gene pyrosequencing. For water mass abbreviations see Table 1.

Figure 6. Redundancy Analysis (RDA) of microbial groups obtained with 454-pyrosequencing and DOM-variables. The filled circles represent the water masses sampled and the stars represent the microbial phylogenetic groups. The direction of the rows indicates the direction of increase in the variable and the length corresponds to DOM-variables. For water mass abbreviations see Table 1. Microbial groups' abbreviations are Acido, Acidobacteria; Actino, Actinobacteria; Flavo, Flavobacteria; Proc, Prochlorococcus; Gemma, Gemmatimonadetes; Phycis, Phycisphaeraceae; Planct, Planctomycetes; A245, AEGAN-245; Rhizo, Rhizobiales; Rhodobac, Rhodobacteraceae; Rhodospi, Rhodospirillales; Ricket, Rickettsiales; Bdello, Bdellovibrionaceae; Nitros, Nitrospinaceae; Myxo, Myxococcales; Altero, Alteromonadales; Oceano, Oceanopirillaceae; Vibrio, Vibrionaceae; Mari, Mariprofundaceae; Verru,

889 Verrucomicrobia; Eury-MGII, Euryarchaeota-MGII; Eury-MGIII, Euryarchaeota-MGIII; Thau,
890 Thaumarchaeota.
891

892 **Table 1.** Physical and chemical characteristics of the main water masses sampled during the cruises BIO-PROF-1 and BIO-PROF-2 along Northwestern of
893 Iberian Peninsule (Fisterra Cape). Euphotic Zone (EZ); Eastern North Atlantic Central Water – Oxygen Minimum Zone (ENACW-OMZ); Mediterrean Water
894 (MW); Labrador Sea Water (LSW); Eastern North Atlantic Deep Water (ENADW), Lower Deep Water (LDW).

895

Water masses	Depth (m)	Temperature (ºC)	Salinity	Oxygen (µmol kg^{-1})	Nitrate (µmol kg^{-1})	Silicate (µmol kg^{-1})	Phospate (µmol kg^{-1})
EZ	≤100	12.47-20.45	35.73-36.11	189.81-269.16	0.10-8.71	0.22-4.40	0.10-0.72
ENACW-OMZ	250-900	10.11-12.92	35.54-36.11	180.47-243.71	7.31-19.50	2.12-8.07	0.51-1.11
MW	1000	3.6-11.42	35.03-36.15	180.58-261.7	13.03-21.44	6.64-12.69	0.72-1.31
LSW	1800-2000	3.56-7.25	34.96-35.21	197.50-261.78	15.54-19.49	9.63-15.23	0.91-1.31
ENADW	2500-2900	2.51-3.50	34.92-35.04	235.13-255.94	14.63-22.96	10.59-35.12	1.02-1.49
LDW	≥4000	2.47-2.54	34.89-34.91	232.03-243.70	18.30-23.23	32.82-47.10	1.24-1.56

896

897

898

899

Table 2. Relative abundance of the major groups of prokaryotes, Thaumarchaeota and Bacteria (% of DAPI) in the different water masses off the Galician coast (Fisterra Cape). For water-mass abbreviations see Table 1.

Water masses	Bacteria	Thaumarchaeota
EZ	54.58±15.08	5.34±2.42
ENACW-OMZ	48.85±5.18	9.52±2.82
MW	43.70±7.03	9.36±3.48
LSW	41.78±5.55	8.22±2.18
ENADW	37.83±5.11	12.98±3.89
LDW	44.51±2.17	14.09±2.17

905 **Table 3.** Multivariate regression analysis (DistLM) of variables contributing to explain the
906 archaeal community structure with "step-wise" selection procedure on the AIC as selection
907 criterion (sequential test). p: represents the significance level; %Variation: corresponds to the
908 percentage of variation explained by each variable; %Cumul: shows the cumulative percentage
909 variance

Depth layer	Variable	Pseudo-F	p	%Var.	%Cumul
Total	FDOM-M	7.1726	**0.001**	13.49	13.49
(n=48)	FDOM-T	2.7069	**0.014**	4.91	18.40
Euphotic Zone					
(EZ) (n=11)	aCDOM254	2.585	**0.015**	22.31	22.31
	FDOM-T	2.4385	**0.040**	12.55	12.55
	aCDOM254	2.3295	**0.042**	11.12	23.66
Intermediate	Depth	2.3541	**0.024**	10.36	34.02
ENACW-OMZ,	sCDOM275-295	2.1236	**0.035**	8.69	42.71
MW)((n=19)	DOC	1.5705	0.131	6.18	48.88
	FDOM-M	1.4421	0.187	5.48	54.37
Deep(LSW,					
NEADW, LDW)	FDOM-M	2.1115	0.042	11.66	11.66
(n=18)					

910

911

Table 4. Multivariate regression analysis (DistLM) of variables that contribute to explain the bacterial community structure with "step-wise" selection procedure on the AIC as selection criterion (sequential test).; p: represents the level of significance; %Var.: corresponds to the percentage of variation explained by each variable; %Cumul.: shows the cumulative variance percentage.

Depth layer	Variable	Pseudo-F	p	%Var.	%Cumul.
Total (n=63)	FDOM-M	10.541	**0.001**	14.73	14.73
	Depth	5.2119	**0.001**	6.81	21.55
	aCDOM365	3.7877	**0.001**	4.73	26.28
	aCDOM340	3.7000	**0.001**	4.42	30.70
	FDOM-T	2.3326	**0.016**	2.72	33.43
	sCDOM275-295	2.3070	**0.012**	2.63	36.06
Euphotic Zone (EZ) (n=18)	Depth	2.4216	**0.016**	13.15	13.15
Intermediate (ENADW-OMZ, MW) (n=25)	sCDOM275-295	4.7230	**0.002**	17.04	17.04
	Depth	3.7751	**0.001**	12.15	29.19
	aCDOM340	1.8321	0.090	5.68	34.87
Deep (LSW, NEADW, LDW) (n=20)	Depth	2.5866	**0.017**	12.57	12.57
	sCDOM275-295	2.4778	**0.044**	11.12	23.69
	aCDOM365	1.8587	0.067	7.94	31.63

Figures:

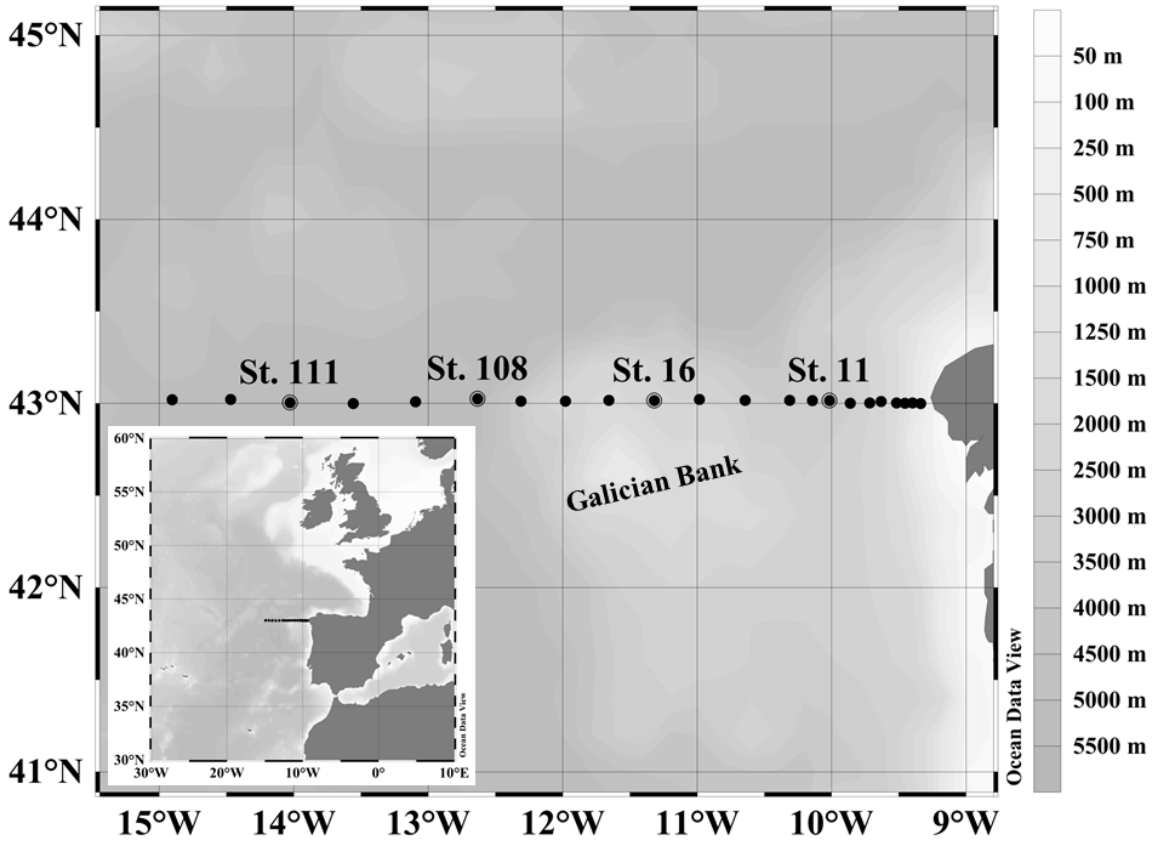

Figure 1

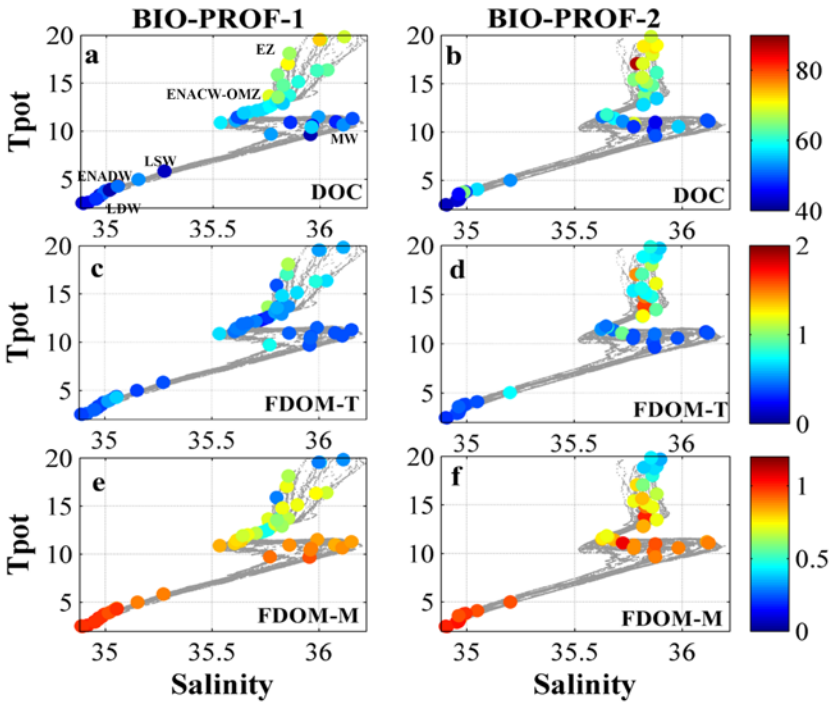
BIO-PROF-1
BIO-PROF-2
a
b
c
d
e
f
EZ
ENACW-OMZ
MW
LSW
ENADW
LDW
DOC
FDOM-T
FDOM-M
Tpot
Salinity
20
15
10
5
35
35.5
36
80
60
40
2
1
0
1
0.5
0

Figure 2

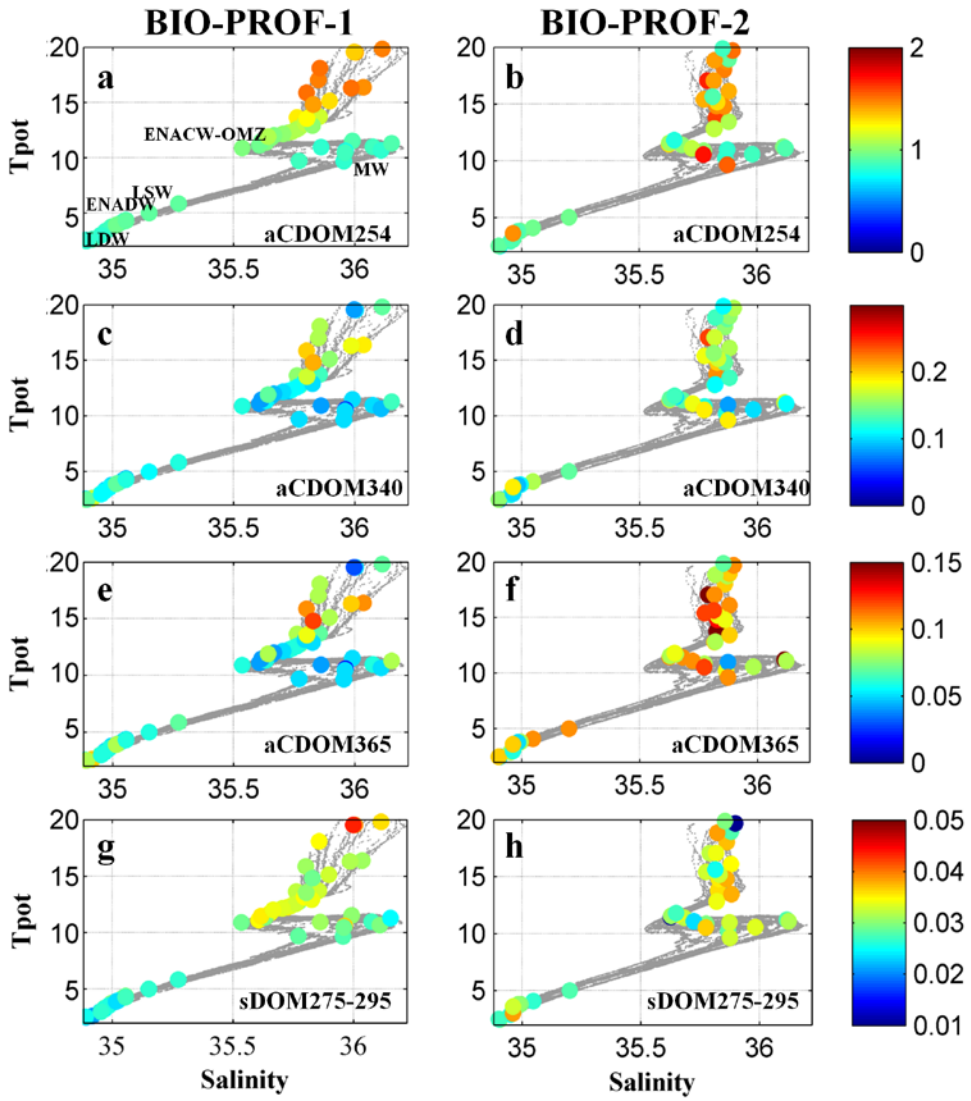
BIO-PROF-1
BIO-PROF-2
a
b
c
d
e
f
g
h
ENACW-OMZ
MW
LSW
ENADW
LDW
aCDOM254
aCDOM340
aCDOM365
sDOM275-295
Tpot
Salinity
20
15
10
5
35
35.5
36
2
1
0
0.2
0.1
0
0.15
0.1
0.05
0
0.05
0.04
0.03
0.02
0.01

Figure 3

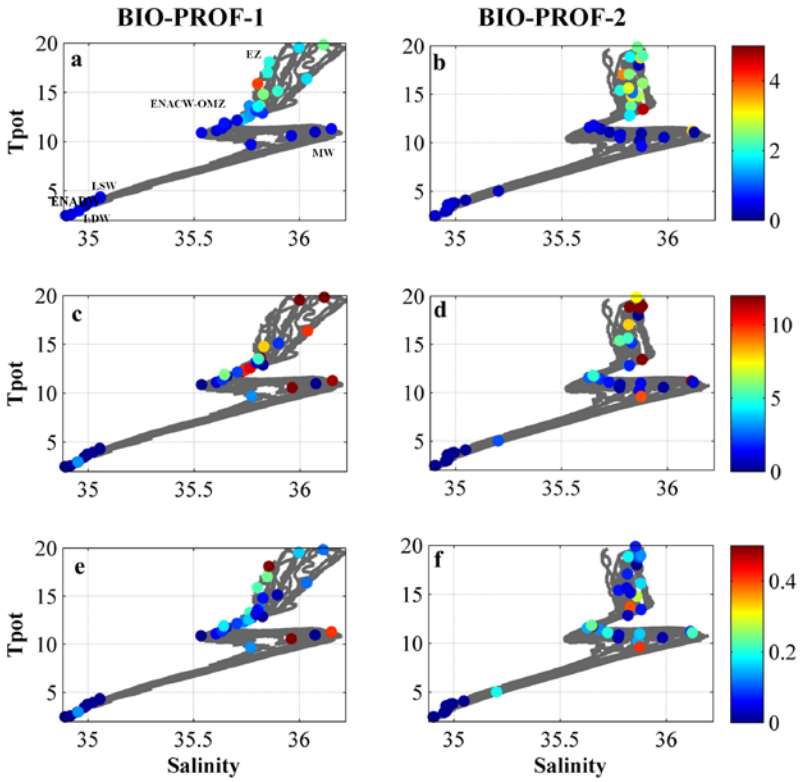
BIO-PROF-1
BIO-PROF-2
a
b
c
d
e
f
EZ
ENACW-OMZ
MW
LSW
ENADW
LDW
Tpot
Salinity
20
15
10
5
35
35.5
36
4
2
0
10
5
0
0.4
0.2
0

Figure 4

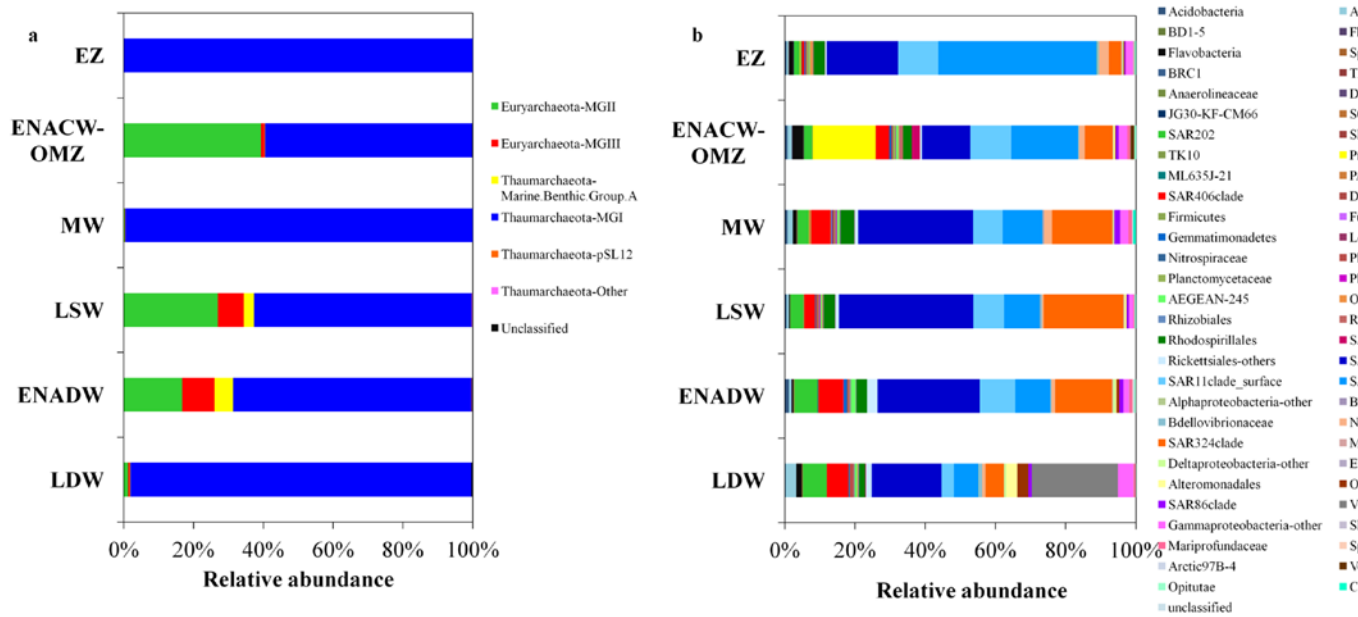
a
EZ
ENACW-OMZ
MW
LSW
ENADW
LDW
0%
20%
40%
60%
80%
100%
Relative abundance
Euryarchaeota-MGII
Euryarchaeota-MGIII
Thaumarchaeota-Marine Benthic Group A
Thaumarchaeota-MGI
Thaumarchaeota-pSL12
Thaumarchaeota-Other
Unclassified
b
EZ
ENACW-OMZ
MW
LSW
ENADW
LDW
0%
20%
40%
60%
80%
100%
Relative abundance
Acidobacteria
BD1-5
Flavobacteria
BRC1
Anaerolineaceae
JG30-KF-CM66
SAR202
TK10
ML635J-21
SAR406clade
Firmicutes
Gemmatimonadetes
Nitrospiraceae
Planctomycetaceae
AEGEAN-245
Rhizobiales
Rhodospirillales
Rickettsiales-others
SAR11clade_surface
Alphaproteobacteria-other
Bdellovibrionaceae
SAR324clade
Deltaproteobacteria-other
Alteromonadales
SAR86clade
Gammaproteobacteria-other
Mariprofundaceae
Arctic97B-4
Opitutae
unclassified

Figure 5

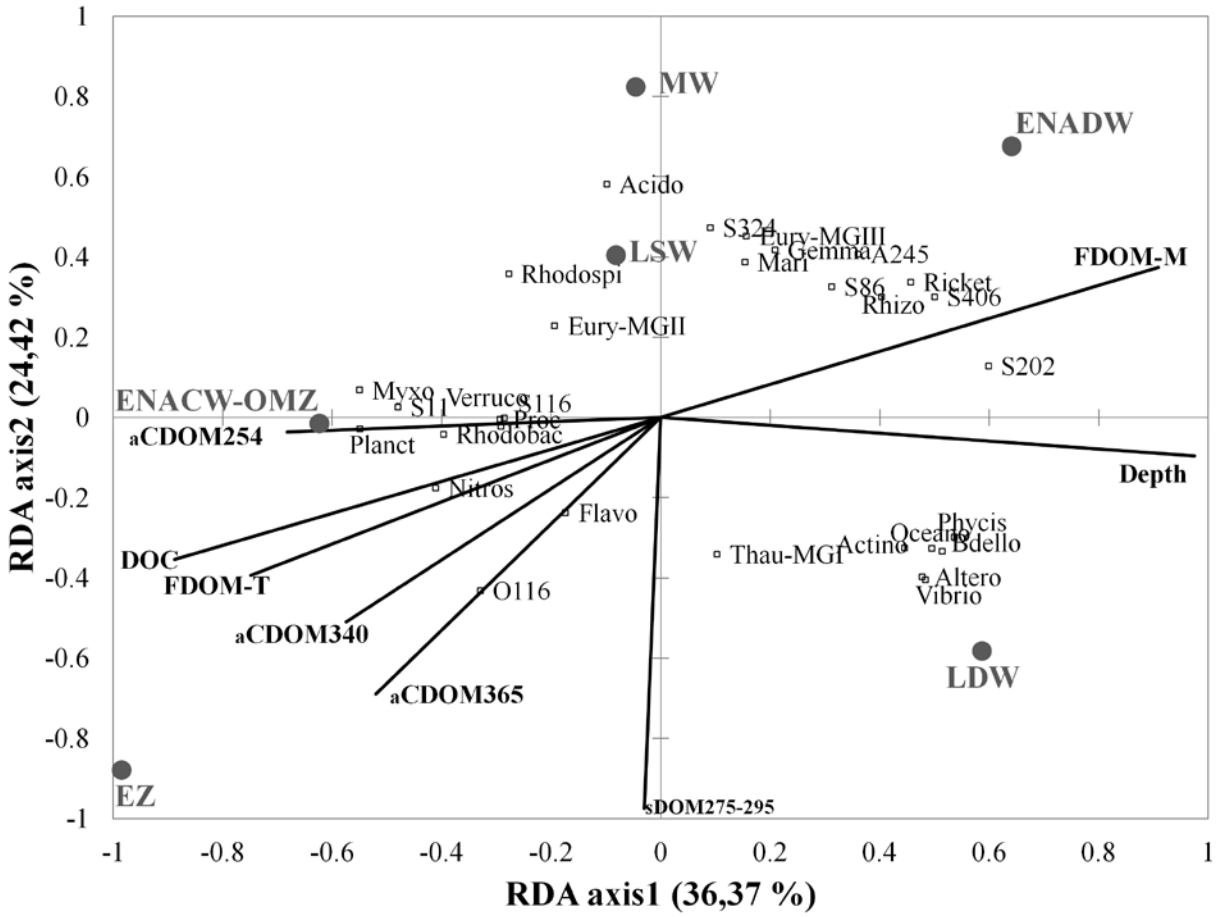
MW
ENADW
LSW
Acido
S324
Eury-MGIII
Gemma
A245
Mari
Rhodospi
S86
Ricket
Rhizo
S406
Eury-MGII
FDOM-M
S202
ENACW-OMZ
Myxo
Verruco
S11
S116
Proc
aCDOM254
Planct
Rhodobac
Depth
Nitros
Flavo
Phycis
Actino
Oceano
Bdello
Thau-MGI
DOC
FDOM-T
Altero
Vibrio
O116
aCDOM340
LDW
aCDOM365
EZ
sDOM275-295
RDA axis2 (24,42 %)
RDA axis1 (36,37 %)
1
0.8
0.6
0.4
0.2
0
-0.2
-0.4
-0.6
-0.8
-1
-1
-0.8
-0.6
-0.4
-0.2
0
0.2
0.4
0.6
0.8
1

Figure 6